http://www.jmaterenvironsci.com/

JMES

The Valorization of a Polymeric Membrane used in Pervaporation Process as Inhibitor of Carbon Steel Corrosion in Hydrochloric Acid Medium

F.Z. Zouhair *, [1], H. Serrar [2], H. Lgaz [3,4], S. Boukhris [2], R. Salghi [4],
H. Oudda [3], S. Jodeh[5], A. Essamri[1]

[1]*Laboratory of Agroresources and Process Engineering, Faculty of Sciences, University Ibn Tofail,B, P14000 Kenitra, Morocco*
[2]*Laboratory of Organic, Organometallic and Theoretical Chemistry, Faculty of Sciences, University Ibn Tofail, 14000 Kenitra, Morocco*
[3]*Laboratory of separation methods, Faculty of Science, University Ibn Tofail PO Box 242, Kenitra, Morocco.*
[4]*Laboratory of Environmental Engineering and Biotechnology, ENSA, Ibn Zohr University, PO Box 1136, 80000 Agadir, Morocco*
[5]*Department of chemistry, An-Najah National University, Nablus, State of Palestine*

F. Z. Zouhair
Fatima.z.zouhair@gmail.com
+212632617747

Abstract

The inhibitor effect of polyvinyl alcohol membrane (PVAM) used in the pervaporation process to dehydrate the bioethanol produced from lignocellulosique materiel was investigated on the corrosion of carbon steel (CS) in 1.0 M HCl solution by weight loss (*WL*), Potentiodynamic polarization (*PDP*) and electrochemical impedance spectroscopy (EIS) measurements. The results show that the inhibition efficiency for the studied compound increased with increasing the inhibitor concentration to attain 88.64 % at the 10^{-5} M of PVAM. Polarization curves showed that PVAM acted as a mixed-type inhibitor in the studied medium. EIS results showed that the change in the impedance parameters (R_{ct} and C_{dl}) with concentration of tested compound is indicative of the adsorption of inhibitor molecules leading to the formation of a protective layer on the surface of the metal. The effect of the temperature on the corrosion behavior with optimum concentration of the inhibitor at a temperature range of 303 to 313 K and the thermodynamic parameters were studied. The adsorption of this compound on carbon steel surface obeys Langmuir's adsorption isotherm.

1. Introduction

The corrosion of carbon steel by aggressive media especially acid solutions causes serious loss on the economy and potential problems in industrial equipment safety [1]. Acids are widely used in industrial processes such as pickling, chemical cleaning and processing, oil recovery and petrochemical industry and other electrochemical systems [2, 3]. Therefore, many different methods have been used in order to protect this metal against corrosion. The use of inhibitors has been found to be one of the best available methods for the protection of metals against corrosion [4]. Organic materials containing functional groups (–OH, –COOH, –NH$_2$, etc.) have particularly been reported as efficient corrosion inhibitors in different corrosive media [5, 6]. However, the utilization of these inhibitors has been restricted for many applications as they are not eco-friendly but toxic and expensive. Many studies about green or eco-friendly environmental inhibitors have been carried out in order to overcome this problem, including polymers that have been investigated as effective corrosion inhibitors for steel [7]. The Literature reveals that the use of polymers as corrosion inhibitors attracted considerable attention recently due to their inherent stability and cost value. Therefore, several polymeric compounds have been successfully investigated applied as potential inhibitors for the corrosion of metals in aggressive media. [8-13]
In this paper, the corrosion inhibition effect of Polyvinylic based membrane has been investigated for CS in 1 M HCl solutions using weight loss, polarization and electrochemical impedance spectroscopy (EIS). This polymeric membrane has already been used as a separative film in pervaporation process for the purification of

ethanol from fermentation broths, as a way of valorization of that membrane after the pervaporation process, in order to develop an ecological and economical bioethanol production process.

2. Materials and methods

2.1. Materials
The steel used in this study is a carbon steel (CS) (Euronorm: C35E carbon steel and US specification: SAE 1035) with a chemical composition:

Table 1. Chemical composition of carbon steel.

	C	Si	Mn	S	Cr	Ti	Ni	Co	Cu	Fe
wt%	0.370	0.230	0.680	0.016	0.077	0.011	0.059	0.009	0.160	Remainder iron

2.2. Synthesis
About 8% (w/w) of PVA was dissolved in distillate water at 85 °C. After casting the solution onto a glass plate, the membrane was dried at 80 °C to evaporate the solvent.

2.3. Solution
The aggressive solutions of 1.0 HCl were prepared by dilution of analytical grade 37% HCl with distilled water. The concentration rage of PVA used was 10^{-5} M to 10^{-8} M.

2.4. Weight loss measurements
Gravimetric measurements were carried out at definite time interval of 6h at room temperature using an analytical balance (precision ± 0.1 mg). The carbon steel specimens used have a rectangular form (length = 1.6 cm, width = 1.6 cm, thickness = 0.07 cm). Gravimetric experiments were carried out in a double glass cell equipped with a thermostated cooling condenser containing 80 mL of non-de-aerated test solution. After immersion period, the steel specimens were withdrawn, carefully rinsed with double distilled water, ultrasonic cleaning in acetone, dried at room temperature and then weighed. Triplicate experiments were performed in each case and the mean value of the weight loss was calculated. The corrosion rate (C_R) and inhibition efficiency η_w (%) were calculated using Eqs. 1 and 2 [14, 15], respectively:

$$CR = \left[\frac{W_b - W_a}{At}\right] \qquad (1)$$

$$\eta_{WL}(\%) = \left[\frac{W^{\circ} - W}{W^{\circ}}\right] \times 100 \qquad (2)$$

Where W_b and W_a are the specimen weight before and after immersion in tested solution, W° and W, are the values of corrosion weight losses of carbon steel in uninhibited and inhibited solutions, respectively, A the total area of carbon steel specimen (cm^2) and t is the exposure time (h).

2.5. Electrochemical measurements

2.5.1 Electrochemical impedance spectroscopy
The electrochemical measurements were carried out using Voltatlab (Tacussel-Radiometer PGZ 100) potentiostate and controlled by Tacussel corrosion analysis software model (Voltamaster 4) at understatic condition. The corrosion cell used had three electrodes. The reference electrode was saturated calomel electrode (SCE). A platinum electrode was used as auxiliary electrode of surface area of 1 cm^2. The working electrode was carbon steel.

All potentials given in this study were referred to this reference electrode. The working electrode was immersed in test solution for 30 min to a establish steady state open circuit potential (E_{ocp}). After measuring the E_{ocp}, the electrochemical measurements were performed. All electrochemical tests have been performed in aerated solutions at 303 K. The EIS experiments were conducted in the frequency range with high limit of 100 KHz and different low limit 0.1 Hz at open circuit potential, with 10 points per decade, at the rest potential after 30 min of acid immersion by applying 10 mV ac voltage peak-to-peak. Nyquist plots were made from these experiments.

The best semicircle can be fit thought that data points in the Nyquist plot using a non-linear least square fit so as to give the intersections with the x-axis.

The inhibition efficiency of the inhibitor was calculated from the charge transfer resistance values using the following equation 3 [16]:

$$\eta_{EIS}(\%) = \left[\frac{R_{ct(inh)} - R_{ct}}{R_{ct(inh)}}\right] \times 100 \tag{3}$$

R_{ct} and $R_{ct(inh)}$ are the charge transfer resistance in absence and in the presence of inhibitor, respectively.

2.5.2 *Potentiodynamic polarization*

The electrochemical behavior of carbon steel sample in inhibited and uninhibited solution was studied by recording anodic and cathodic potentiodynamic curves. Measurements were performed in the 1.0 M HCl solution containing different concentrations of the tested inhibitor by changing the electrode potential automatically from 800 to -200 mV *vs* corrosion potential at a scan rate of 2 mV.s^{-1}. The linear Tafel segments of anodic and cathodic curves were extrapolated to corrosion potential to obtain corrosion current densities (I_{corr}). From the polarization curves obtained, the corrosion current (I_{corr}) was calculated by curve fitting using the equation.

$$I = I_{corr}\left[\exp\left(\frac{2.3\Delta E}{\beta_a}\right) - \exp\left(\frac{2.3\Delta E}{\beta_c}\right)\right] \tag{4}$$

The inhibition efficiency was calculated from the measured I$_{corr}$ values using the relationship [17]:

$$\eta_{PDP}(\%) = \left[1 - \frac{i_{corr}}{i_{corr}^{\circ}}\right] \times 100 \tag{5}$$

i_{corr}° and i_{corr} are the corrosion current density in the absence and the presence of the inhibitor, respectively.

3. Results and discussion

3.1 Weight loss tests

The inhibition efficiency η_w (%) and corrosion rate (C_R) obtained from the weight loss measurements at different concentrations of PVAM in 1.0 M HCl solution are shown in Table 2. The inhibition efficiencies increase and the corrosion rate decreases obviously with increasing the concentration of PVAM, which can be explained by the adsorption of PVAM on the carbon steel surface in 1.0 M HCl leading to the formation of the protective film. The maximum efficiency reaches 88.64 % at the highest concentration.

Table 2. Corrosion parameters obtained from weight loss measurements for carbon steel in 1.0 M HCl containing various concentrations of **PVAM** at 303 K.

Inhibitor	Concentration (M)	C_R (mg cm^{-2} h^{-1})	η_w (%)	Θ
Blank	1.0	1.083	-	-
PVAM	10^{-5}	0.123	88.64	0.886
	10^{-6}	0.179	83.47	0.834
	10^{-7}	0.196	81.90	0.819
	10^{-8}	0.275	74.61	0.746

3.2 Effect of temperature

Temperature has a great effect on the corrosion phenomenon. Generally the corrosion rate increases with increasing temperature [18]. In order to obtain additional insights on the corrosion process of the PVAM on carbon steel in 1.0 M HCl, the influence of the temperature on the corrosion behavior of steel/acid interface in the presence and absence of the 10^{-5} M of PVAM was investigated using weight loss method at the temperature range of 303-333 K during 6h of immersion.
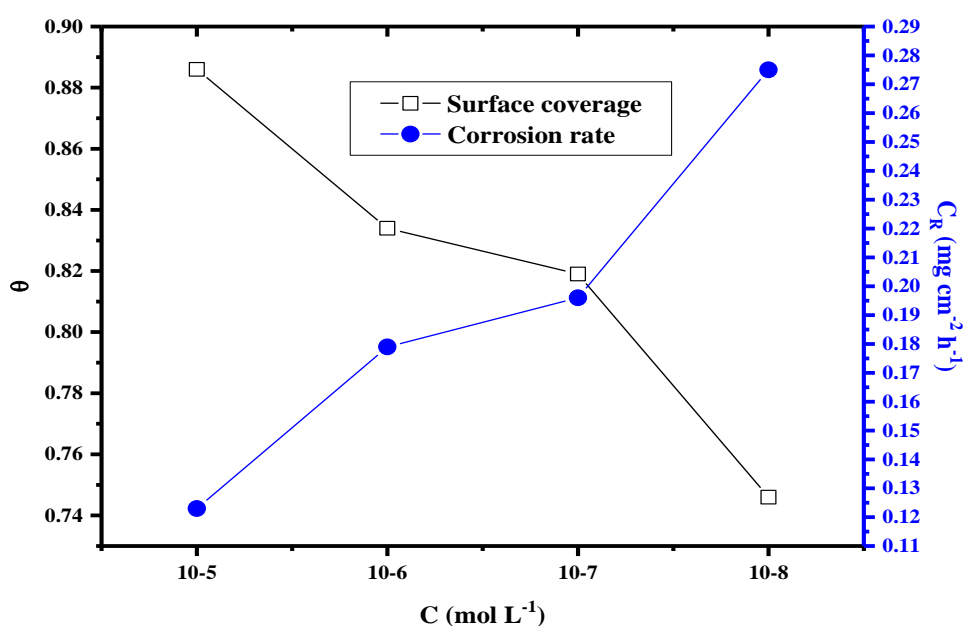
Figure 1. Relationship between the corrosion rate, the inhibition efficiency and **PVAM** concentrations for steel after 6 h immersion in 1.0 M HCl at 303 K

Table 3: C_R and η_w % obtained from weight loss measurements of carbon steel in 1 M HCl containing 10^{-5} M of **PVAM** at different temperatures.

Inhibitors	Temperature (K)	C_R (mg cm^{-2} h^{-1})	η_w (%)	Θ
Blank	303	1.083	-	-
	313	2.474	-	-
	323	5.079	-	-
	333	10.087	-	-
PVAM	303	0.123	88.64	0.886
	313	0.467	81.12	0.811
	323	1.346	73.50	0.735
	333	3.544	64.87	0.648

The corresponding data are shown in Table 3. This Table clearly shows that corrosion rate (C_R) increases with increasing temperature, while the inhibition efficiency decreases with increasing temperature from 303 to 333K. This indicates that at higher temperature, the dissolution of carbon steel predominates on adsorption of the inhibitor at the metal surface. This can be explained by the decreases of the strength of adsorption process at high temperature [19]. The values of activation energy E_a, the change in activation enthalpy ΔHa and the change in activation entropy ΔS$_a$ were estimated using Arrhenius equation and transition state equation (6 and 7) [20, 21].

$$I_{corr} = A \exp\left(\frac{-E_a}{RT}\right) \tag{6}$$

$$I_{corr} = \frac{RT}{Nh} \exp\left(\frac{\Delta S_a}{R}\right) \exp\left(-\frac{\Delta H_a}{RT}\right) \tag{7}$$

Where *h* is Planck's constant, *N* is Avogadro's number, ΔS$_a$, is the change in entropy of activation an ΔH$_a$ is the change in enthalpy of activation.

Plots of Ln (I_{corr}) vs. 1000/T and Ln (I_{corr}/T) vs. 1000/T gave straight lines with slopes of $-E_a$/R and $-\Delta h_a$/R, respectively. The intercepts were A and [Ln (R/Nh) + (ΔS_a/R)] for the Arrhenius and transition state equations, respectively. Fig. 2 and 3 represent the data plots of Ln (I_{corr}) vs. 1000/T and Ln (I_{corr}/T) vs. 1000/T in the absence and presence of 10^{-5} M PVAM. The calculated values of the activation parameters are tabulated in Table 4.
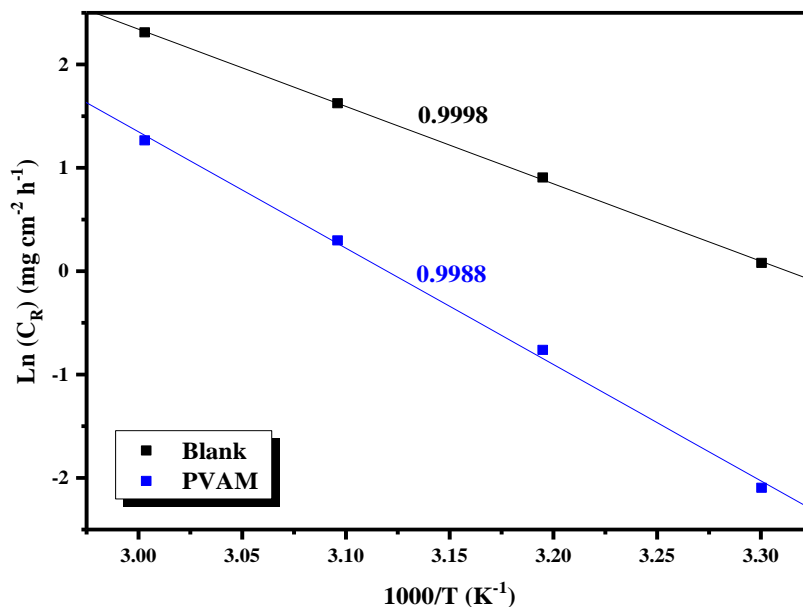
Figure 2. Arrhenius plots for MS in 1 M HCl in the absence and presence of 10^{-5} M of inhibitors at different temperatures.

The data listed in the Table 3 show that the value of E_a for PVAM is higher than that obtained for 1.0 M HCl solution and consequently the rate of corrosion decreases [22].

Table 4. Activation parameters for carbon steel corrosion in 1M HCl in the absence and presence of 10^{-5} M of inhibitor at different temperatures.

Inhibitor	E_a (kJ/mol)	ΔH_a (kJ/mol)	ΔS_a (J mol-1 K-1)	E_a - ΔH_a
Blank	62.20	59.56	-47.48	2.64
10^{-5}M PVAM	93.55	90.91	38.32	2.64

The increase in the apparent activation energy indicated the formation of energy barrier for carbon steel dissolution in presence of PVAM [23]. On the other hand, the positive sign of ΔH_a shows that the corrosion process of carbon steel is an endothermic phenomenon [24]. The change in entropy of activation, ΔS_a, in the absence of the inhibitor is negative, indicating that the rate-determining step for the activated complex is the association rather than the dissociation step, while in the presence of the inhibitor, ΔS_a is positive, which implies that the adsorption process is accompanied by an increase in entropy, which is driving force for the adsorption of inhibitor onto the carbon steel surface [25]. We can notice that E_a and ΔH_a values vary in the same way permitting to verify the known thermodynamic reaction between the E_a and ΔH_a as shown in Table 4 [26]:

$$\Delta H_a = E_a - RT \tag{8}$$
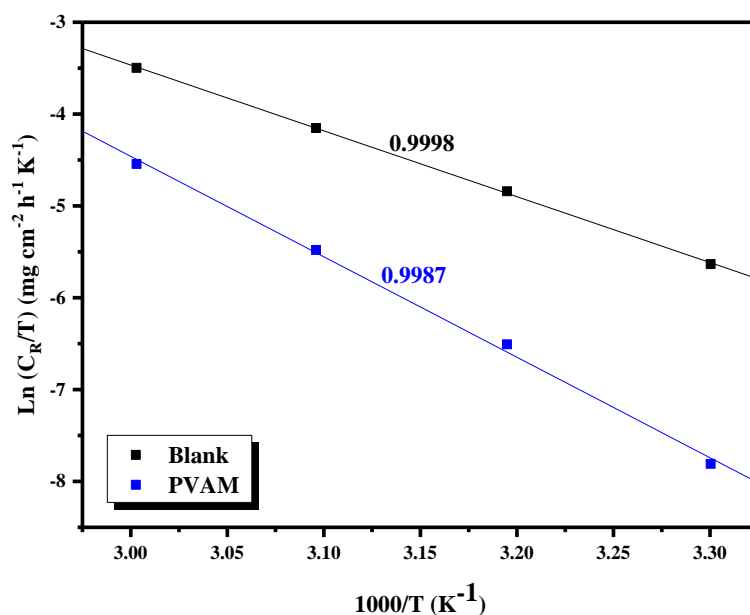
Figure 3. Transition state plots for the inhibition of corrosion of MS in 1M HCl in the absence and presence of 10^{-5} M of inhibitors at different temperatures.

3.3 Polarization results

In order to have a better understanding of the role of the inhibitor in biasing anodic and cathodic reactions, a potentiodynamic polarization study has been made. Figure 4 shows anodic and cathodic polarization plots of carbon steel in 1.0 M HCl in the absence and in the presence of PVAM inhibitor of different concentrations at 303 K. Table 5 shows the electrochemical corrosion parameters such as a corrosion potential (*E* versus *SCE*), corrosion current density (I_{corr}) and the inhibition efficiency (*IE%*).
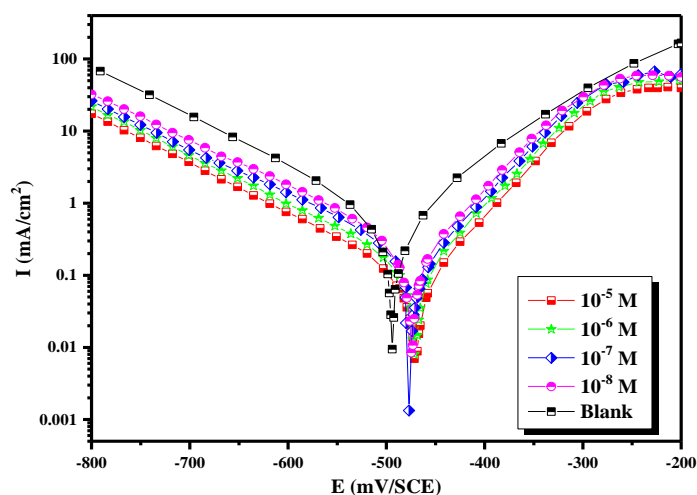
Figure 4. Polarisation curves of carbon steel in 1.0 M HCl for various concentrations of **PVAM** at 303K.

The data in the Table 5 show that the PVAM effectively decreases the corrosion current density of the carbon steel, even when added in small concentrations. Inhibition efficiency increases with the increase in the inhibitor concentration up to an optimum value. The presence of inhibitor does not cause any significance shift in the E_{corr} value. This implies that the inhibitor, PVAM, acts as a mixed type inhibitor, affecting both anodic and cathodic reactions [27]. According to Riggs and others [28], if the displacement in corrosion potential is more

than ± 85 mV/SCE with respect to the corrosion potential of the blank, the inhibitor can be considered as a cathodic or anodic type. But the maximum displacement in the present work is 27 mV/SCE, which further indicates the mixed type of our inhibitor. Figure 4 indicates that the cathodic polarization curves are parallel and cathodic Tafel slope βc changes slightly with the increase in the inhibitor concentration. This suggests that the mechanism of the corrosion reaction is not affected by the presence of inhibitor [29, 30]

Table 5. Polarization data of carbon steel in 1.0 M HCl without and with various concentrations of **PVAM** at 303 K.

Inhibitor	Concentration (M)	$-E_{corr}$ (mV/SCE)	$-\beta c$ (mV dec^{-1})	I_{corr} (μA cm^{-2})	η_{Tafel} (%)	Θ
Blank	1.0	496	162.00	564	-	-
PVAM	10^{-5}	469	157.16	77.32	86.29	0.862
	10^{-6}	473	163.79	101.97	81.92	0.819
	10^{-7}	477	161.96	147.44	73.85	0.738
	10^{-8}	473	159.58	191.31	66.08	0.660

3.4. Electrochemical impedance spectroscopy measurements
The experimental results obtained from *EIS* measurements for the corrosion of carbon steel in the absent and presence of inhibitor at 303 K are summarized in Table 6. The impedance spectra for carbon steel in 1.0 M HCl without and with various concentrations of PVAM are presented as Nyquist plots in Figure 5. These diagrams have similar shape throughout all tested concentrations, indicating that almost no change in the corrosion mechanism occurs due to the inhibitor addition [31]. The high frequency loops are not perfect semicircles which can be attributed to the frequency dispersion as a result of the roughness and inhomogeneous of electrode surface [32].
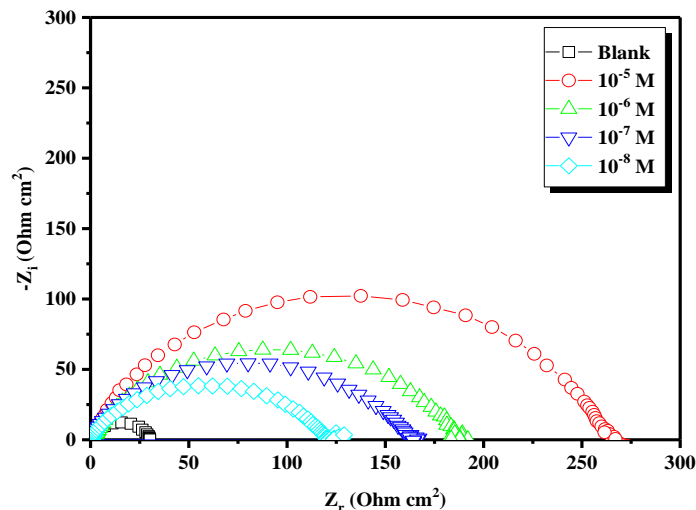
Figure 5. Nyquist diagrams for carbon steel in 1.0 M HCl at different concentrations of **PVAM** at 303 K

It should be noted that the best fit of experimental data to this single time constant model was obtained using a constant phase element (CPE) rather than ideal capacitor. The electrical equivalent circuit model shown in Figure 7 was used to analyze the obtained impedance data. The model consists of the solution resistance (Rs), the charge-transfer resistance of interfacial corrosion reaction (R_{ct}) and the constant phase angle element (*CPE*). Excellent fit with this model was obtained with our experimental data. As an example, the Nyquist plots of both experimental and simulated data of carbon steel in 1.0 M HCl solution containing 10^{-6} M of PVAM are shown in Figure 6. It is clear that the measured impedance plot is in accordance with that calculated by the used equivalent circuit model. Various parameters such as charge transfer resistance (R_{ct}), solution resistance (Rs),

double layer capacitance (C_{dl}) and inhibition efficiency (η_{EIS}) were calculated and listed in Table 6. As it can be observed from this Table, it was revealed that R_{ct} values increases obviously while C_{dl} reduces with increasing of the concentration of PVAM. Which can results from a decrease in local dielectric constant and/or an increase in the thickness of the electrical double layer, suggested that the inhibitor species function by adsorption at the metal/solution interface [33]. In Table 6 the double layer capacitance C_{dl} was calculated by Eq (9):

$$C_{dl} = \sqrt[n]{Q \times R_p^{1-n}} \tag{9}$$

Where Q and n are *CPE* (Constant Phase Element) parameters. The parameter ''n'' of the *CPE* is an indicator of electrode surface roughness or heterogeneity and parameter ''Q'' is considered to be the *CPE* admittance.

According to Table 6, as the concentration of PVAM increase the double layer capacitance decreases. The double layer capacitance can also be expressed in the Helmholtz model by Eq. (10)

$$C_{dl} = \frac{\varepsilon_0 \varepsilon}{\delta} S \tag{10}$$

Where δ is the thickness of electrical double layer, S is the surface of the electrode, ε_0 is the permittivity of vacuum and ε is the medium dielectric constant. The decrease in C_{dl} may be interpreted either by a decrease of local dielectric constant (ε) or increase of electrical double layer thickness (δ) on the metal surface [34].

The inhibition efficiency increasing with increasing the corrosion inhibitor concentration and the maximum inhibition efficiency reached up to 88.66 %, which further confirms that the PVAM exhibits very good inhibitive performance for carbon steel in 1.0 M HCl.

Table 6. Impedance parameters for corrosion of carbon steel in 1.0 M HCl in the absence and presence of different concentrations of **PVAM** at 303 K.

Inhibitor	Concentration (M)	R_{ct} (Ω cm^2)	n	$Q \times 10^{-4}$ (s^n Ω^{-1}cm^{-2})	C_{dl} (μF cm^{-2})	η_z (%)	Θ
Blank	1.0	29 .35	0.91	1.7610	91.60	-	-
PVAM	10^{-5}	258.9	0.85	0.3987	17.79	88.66	0.886
	10^{-6}	182.7	0.87	0.4822	23.78	83.93	0.839
	10^{-7}	152.3	0.84	0.6242	25.71	80.73	0.807
	10^{-8}	114.1	0.83	0.8563	33.18	74.28	0.742
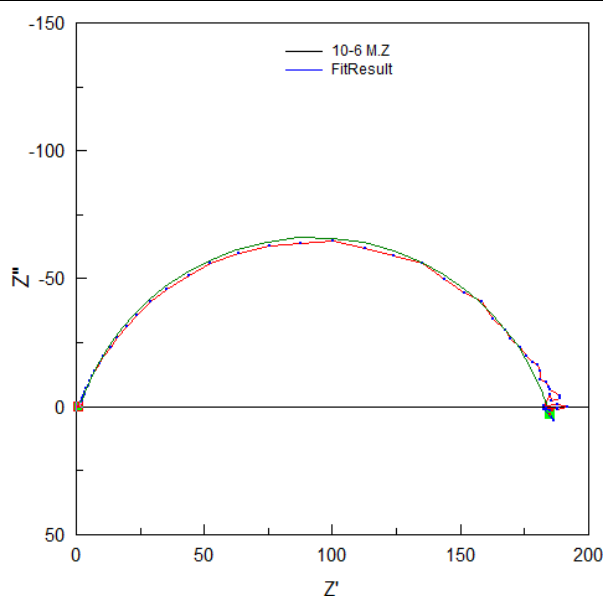
Figure 6. EIS Nyquist plots for carbon steel in 1.0 M HCl with 10^{-6} M **PVAM** interface: dotted lines experimental data; dashed line calculated.
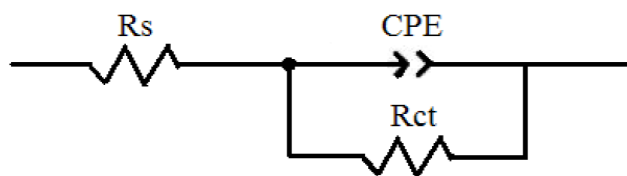
Figure 7. Equivalent electrical circuit corresponding to the corrosion process on the carbon steel in hydrochloric acid.

3.5. Adsorption considerations

The mechanism of the interaction between inhibitor and the electrode surface can be explained using adsorption isotherms. Several adsorption isotherms were tested and the Langmuir adsorption isotherm was found to provide best description of the adsorption behavior of the investigated inhibitor. The Langmuir isotherm is given by the equation [35]:

$$\frac{C_{inh}}{\theta} = \frac{1}{K_{ads}} + C_{inh} \qquad \text{With} \qquad \Delta G°_{ads} = -RT\ln(K_{ads} \times 55.5)$$

Where C_{inh} is the concentration of inhibitor, K the adsorptive equilibrium constant, ΔG_{ads} is the standard free energy of adsorption reaction, R is the universal gas constant, T is the absolute temperature in Kelvin, θ is the fraction of the surface covered as follows $\theta = IE$ (%)/100 and the value of 55.5 is the concentration of water in the solution in mol/L. Figure 8 shows the dependence of the ratio C_{inh}/θ as function of C_{inh}. Linear plot is obtained from slope and correlation coefficient close to 1.
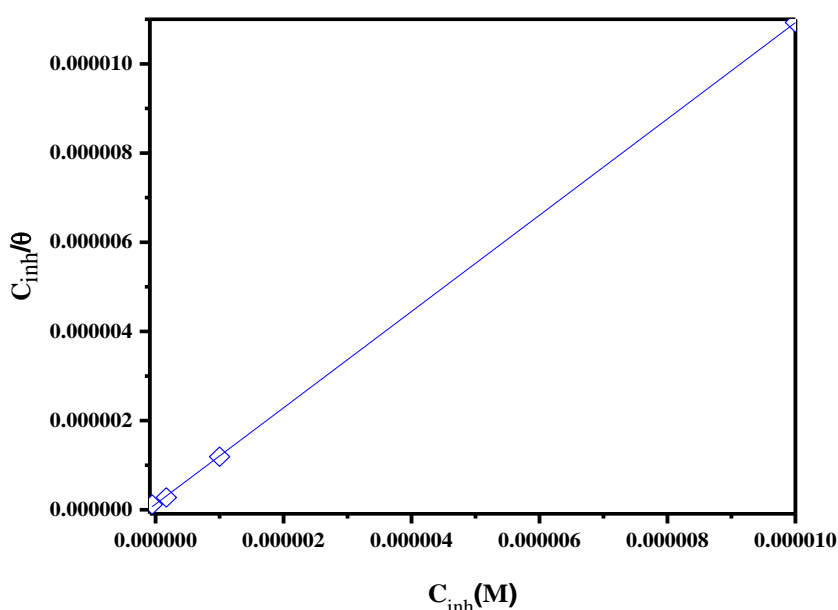
Figure 8. Langmuir adsorption of **PVAM** on the carbon steel surface in 1.0 M HCl solution at 303K.

The value of K_{ads} was found to be 7779800 M⁻¹ (Table 7). The relatively high value of adsorption equilibrium constant reflects the high adsorption ability of PVAM on carbon steel surface [36]. The value of $\Delta G°_{ads}$ was calculated as -50.06 KJ mol⁻¹. The negative value of $\Delta G°_{ads}$ indicates the spontaneity of adsorption process and the stability of adsorbed layer on the carbon steel surface [37]. It is well known that the values of $\Delta G°_{ads}$ of the order of -20 KJ mol⁻¹ or lower indicate a physisorption, those of order of -40 kJ mol⁻¹ or higher involve charge sharing or transfer from the inhibitor molecules to the metal surface to form a coordinate type of bond (chemisorption) [38-40]. On the other hand, the adsorption phenomenon of an organic molecule is not

considered only as a purely physical or chemical adsorption phenomenon [41-42]. A wide spectrum of conditions, ranging from the dominance of chemisorption or electrostatic effects, arises from other adsorptions experimental data [14]. The value of -53.92 kJ mol^{-1} may suggest the predominance of the chemisorption mode.

Table 7. Thermodynamic parameters for the adsorption of **PVAM** in 1.0 M HCl on the Carbon steel at 303K

Inhibitor	Slope	$K_{ads}(M^{-1})$	R^2	ΔG°_{ads} (kJ/mol)
PVAM	1.06	7779800	0.9999	-50.06

Conclusion
The results of this work show that:
- The inhibition efficiency of polyvinyl alcohol membrane (PVAM) increases with the concentration and reached 88.64 % at 10^{-5} M; we could say that PVA membrane is a good corrosion inhibitor at low concentrations.
- Polarization study showed that the studied compound was mixed type inhibitor.
- The weight loss, polarization curves and electrochemical impedance spectroscopy were in good agreement.
- The inhibition efficiency decreased with increasing temperature and their addition led to an increase of the activation corrosion energy.
- Adsorption of the inhibitor on the carbon steel surface from 1.0 M HCl followed the Langmuir isotherm.
- These results lead us to conclude that polyvinylic based membrane is demonstrated as a good inhibitor for the corrosion of carbon steel in the studied medium, which can be a promising way for the valorization of those polymeric membrane already used in the pervaporation process as a separative films.

Reference

1. Behzadnasab M., Mirabedini S.M., Esfandeh M., *Corros. Sci.* 75 (2013) 134–141.
2. Karthikaiselvi R., Subhashini S., Rajalakshmi R., *Arab. J. of Chemistry.* 5 (2012) 517–522.
3. Salghi R., Anejjar A., Benali O., Al-Deyab S. S., Zarrouk A., Jama C., Hammouti B., *Int. J. Electrochem. Sci.*, 9 (2014) 5315 – 5327.
4. Eddy, N.O., Ekwumemgbo, P.A., Mamza, P.A.P., *Green Chem. Lett. Rev*. (2009)a 2 (4), 223–2.
5. Muller B., Forster I., Klager W., *Prog. Org. Coat*. 31 (1997) 229.
6. El-Sayed A., *Corrosion. Prev. Contr* 43 (1996) 27.
7. Olivares, O., Likhanova, N.V., Gomez, B., Navarrete, J., Llanos- Serrano, M.E., Arce, E., Hallen, J.M., *Appl. Surf. Sci.* 252 (2006) 2894–2909.
8. Schweinsberg, D.P., Hope, G.A., Trueman, A., Otieno-alego, V., *Corros. Sci.* 38 (4) (1996) 587–599.
9. Abd El Rehim, S.S., Sayyah, S.M., El-Deeb, M.M., Kamal, S.M., Azooz, R.E., Mater. *Chem. Phys.* 123 (2010) 20– 27.
10. Mostafa Abo El-Khair, B., *Surf. Coat. Technol*, 27 (1986) 317–324.
11. Gandhi, S., Abiramipriya, P., Pooja, N., Juliat Latha Jeyakumari, J., Yelil Arasi, A., Dhanalakshmi, V., Gopinathan Nair, M.R., Anbarasan, R., *J. Non-Cryst. Solids*, 357 (2011) 181–185.
12. Umoren S.A., Ogbobe O., Igwe I.O., Ebenso E.E., *Corros. Sci*, 50 (2008) 1998–2006.
13. Ashassi-Sorkhabi H., Ghalebsaz-Jeddi N., Hashemzadeh F., Jahani H., *Electrochim. Acta*, 51 (2006) 3848–3854.
14. Ahamad I., Prasad R., QuraishiM.A., *Corros. Sci.*, 52 (2010) 933.
15. Bentiss F., Outirite M., Traisnel M., Vezin H., Lagrenée M., Hammouti B., Al-Deyab S.S., Jama C., *Int. J. Electrochem. Sci.*, 7 (2012) 1699.
16. Zarrok H., Zarrouk A., Hammouti B., Salghi R., Jama C., Bentiss F., *Corros. Sci.*, 64 (2012) 243.
17. Obot I. B., Obi-Egbedi N.O., *Curr. Appl. Phys.*, 11 (2011) 382.

18. Zarrok, H., Zarrouk, A., Salghi, R., Ramli, Y., Hammouti, B., Al-Deyab, Oudda, H., *Int .J. Electrochem. Sci*, 7 (2012) 8958-8973.
19. Zarrok, H., Zarrouk, A., Hammouti, B., Salghi, R., Jama, C., & Bentiss, F., *Cor. Sci* 64 (2012) 243-252.
20. Anejjar A., Salghi R., Zarrouk A., Benali O., Zarrok H., Hammouti B., Ebenso E.E., *J. Assoc. Arab Univers. Bas. Appl. Sci.*, 15 (1) (2014) 21.
21. Salghi R., Anejjar A., Benali O., Al-Deyab S. S., Zarrouk A., Errami M., Hammouti B., Benchat N., *Int. J. Electrochem. Sci.*, 9 (6) (2014) 3087.
22. Messaadia L., ID EL mouden O., Anejjar A., Messali M., Salghi R., Benali O., Cherkaoui O., Lallam A., *J. Mater. Environ.* 6 (2) (2015) 598-606.
23. Quraishi M.A., Verma C., Olasunkanmi L. O., Ebenso E., *RSC Adv.* (2015) DOI: 10.1039/C5RA16982H.
24. Guan N.M., Xueming L., Fei L., *Mater. Chem. Phys.* 86 (2004) 59.
25. Li X., Deng S., Fu H., Mu G., *Corros. Sci.*, 50 (2008) 2635.
26. Zarrouk A., Warad I., Hammouti B., Dafali A., Al-Deyab S.S., Benchat N., *Int. J. Electrochem. Sci.*, 5 (2010) 1516.
27. Jayaperumal D., Mater. *Chem. Phys.*, 119 (2010) 478.
28. Li W., He Q., Zhang S., Pei C., Hou B., *J. Appl. Electrochem.*, 38 (2008) 289.
29. Ehteshamzadeh M., Jafari A.H., Naderi E., Hosseini M.G., *Mater. Chem. Phys.*, 113 (2009) 986.
30. Ateya B.G., El-Khair M.B.A., Abdel-Hamed I.A., *Corros. Sci.*, 16 (1976) 163.
31. Labjar N., Lebrini M., Bentiss F., Chihib N.E., El Hajjaji S., Jama C., *Mater. Chem. Phys.* 119 (2010) 330.
32. Lebrini M., Lagrenee M., Vezin H., Traisnel M., Bentiss F., *Corros. Sci.* 49 (2007) 2254.
33. Khaled K.F., Hackerman N., *Mater. Chem. Phys.* 82(2003) 949.
34. Christov M., Popova A., *Corros. Sci*, 46 (2004) 1613.
35. Langmuir I., *J. Am. Chem. Soc.* 39 (1947) 1848.
36. Guan N.M., Xueming L., Fei L., *Mater. Chem. Phys.*, 86 (2004) 59.
37. Verma C., Ebenso E., Obot I. B. and Olasunkanmi L., Quraishi M. A., *RSC Adv.*, 19 (2016) 15279-16114, DOI: 10.1039/C5RA27417F.
38. Lebrini M., Robert F., Roos C., *Int. J. Electrochem. Sci.* 5 (2010) 1698.
39. Moretti G., Quartaronr G., Tassan A., Zingales A., *Electrochim. Acta*, 41 (1996) 1971.
40. Growcock F. and Lopp V. R., *Corrs.Sci.*,(1988) 28, 397.
41. Ali S.A., Saeed M.T., Rahman S.U., *Corros. Sci.* 45 (2003) 253.
42. Migahed M.A., *Mater. Chem. Phys.* 93 (2005), 48.

(2017) ; http://www.jmaterenvironsci.com